PHYSICAL REVIEW B VOLUME 10, NUMBER 10 15 NOVEMBER 1974

Photoconductivity and electron transport parameters in liquid and solid xenon*

U. Asaf and I. T. Steinberger

Racah Institute of Physics, Hebrew University, Jerusalem, Israel

(Received 23 July 1974)

In photoconductivity excitation spectra of liquid xenon a threshold at 9.20 eV and a dip at 9.45 eV, very near to the peak of the competing $n = 1$ [$\Gamma(1/2)$] exciton transition, were observed. From the results the $\Gamma(3/2)$ band gap was determined to be $E_G = 9.22 \pm 0.01$ eV. This value is very near to the estimate (9.24 eV) based on the density change of xenon on melting. Combining the value for E_G with the measured position of the $n = 2$ [$\Gamma(3/2)$] exciton peak yielded an exciton binding energy $G = 1.08$ eV and effective exciton reduced mass $m^* = 0.27$ (in units of electron mass). Using m^* and published results of the bulk modulus and mobility, the following parameters were obtained for liquid Xe at 163 °K: relaxation time $\tau = 3.4 \times 10^{-13}$ sec, mean free path $L = 3.3 \times 10^{-6}$ cm, absolute value of scattering length $|a| = 4.2 \times 10^{-9}$ cm, absolute value of conduction-band deformation potential $|E_{1CB}| = 1.0$ eV. On the other hand, for solid xenon at 161 °K $\tau = 8.0 \times 10^{-13}$ sec, $L = 7.1 \times 10^{-6}$ cm, $|a| = 3.8 \times 10^{-9}$ cm, and $|E_{1CB}| = 0.93$ eV. The significance of the results is discussed.

I. INTRODUCTION

The liquid rare gases Xe, Kr, and Ar seem to be the simplest group of noncrystalline semiconductors. They exhibit high electron mobilities[1] (of the order of 10^3 cm^2/V sec). The absorption spectra of rare-gas liquids containing atomic[2,3] or molecular[4] impurities are similar to those of the corresponding solids[5,6] and show prominent absorption due to the presence of the impurity. These absorption bands are attributed to bound Wannier excitons. The reflection spectrum of pure liquid xenon[7,8] is almost as rich in excitonic structure {e.g., $n=1$ [$\Gamma(\frac{3}{2})$] and $n=1$ [$\Gamma(\frac{1}{2})$] excitons} as that of the solid.[9-11] It is particularly significant that the $n=2$ [$\Gamma(\frac{3}{2})$] Wannier exciton was clearly observed in the liquid as well. In fact, liquid rare gases seem to be the only noncrystalline materials where Wannier excitons have ever been observed. This fact is closely connected with the existence of a quasifree excess-electron state[12] in these liquids, i.e., that of a proper conduction band. The similarity between the solid and the liquid goes even further[13]: the positions of the $n=1$ [$\Gamma(\frac{3}{2})$], $n=2$ [$\Gamma(\frac{3}{2})$], and $n=1$ [$\Gamma(\frac{1}{2})$] exciton peaks in solid Xe have a linear dependence on density, and the extrapolation of the straight line fits well the exciton positions of the liquid.

The forbidden band, separating the uppermost valence band from the first conduction band, is not displayed in condensed rare gases as an absorption edge, since strong absorption due to excitons ($\alpha \approx 10^6$ cm^{-1}) masks completely the band-to-band transitions. Traditionally, the width of the energy gap E_G has been determined by extrapolating[9-11, 13-15] observed Wannier series $E_n = E_G - G/n^2$ to $n=\infty$. This procedure has been recently corroborated[16] by observing the onset of photoconductivity in solid Xe due to band-to-band transitions.

In liquid xenon only the $n=1$ and $n=2$ exciton peaks of the $\Gamma(\frac{3}{2})$ series are observed and thus the reflection spectrum yields only a rough estimate of the band gap. Employing photoconductivity techniques is an obvious alternative. However, the only published data[17] on the photoconductivity of liquid xenon seem to be complicated by the presence of impurities and by inconvenient geometry. The response obtained is quite different from that observed in the solid,[16] and the band gap deduced from these results is unreasonably narrow (8.9 eV). It was therefore considered necessary to measure photoconductivity excitation spectra in this material with improved techniques. The results point to a band gap of $E_G = 9.22$ eV. They clearly exhibit the interplay and competition between creation of $\Gamma(\frac{1}{2})$ excitons and photoconductivity. Combination of E_G with results on the mobility and the bulk modulus lead to an evaluation of a set of electron transport parameters in liquid xenon, including the scattering length.

II. EXPERIMENTAL ARRANGEMENT

The optical system has been described previously.[13] Matheson research grade xenon gas was used (99.995% pure, containing less than 50-ppm Kr, less than 5-ppm O_2, and less than 5-ppm N_2) without further purification. The gas was condensed in a closed cell[16] having a MgF_2 front window. The inner surface of this window was covered by a couple of evaporated gold electrodes, in the shape of interlaced combs. This electrode arrangement was chosen in order to obtain relatively large currents even if the resistivity was high. The combs are equivalent to two parallel electrodes of 60-mm length with a spacing of 0.5 mm in between them. Complications due to electron trapping by impurities[17] and photoelectric effects associated with the window[17] were avoided in this setup. The geometry prevents emission of electrons from the xenon sample to the surrounding vacuum. Photoemission from the sample into the MgF_2 window is unlikely, but cannot be ruled out completely. As previously, direct voltages (up to 200 V) were applied and the currents were measured by an electrometer amplifier.

III. RESULTS

Figure 1 represents the photocurrent of solid and liquid Xe as a function of photon energy, normalized to equal numbers of incident photons. The similarity between the behaviors of the solid and of the liquid is obvious. Below about 9.2 eV very little photocurrent was seen in any case, with a peak at about 8.6 eV, corresponding to the $n=1$ $[\Gamma(\frac{3}{2})]$ exciton transition. The magnitude of the currents in this region was dependent in a complicated manner on previous light irradiations and voltage applications on the sample, thus making it likely that they are due to release of previously trapped electrons by excitons. The currents in this region were never more than 10% of the current observed above (by, say, 0.2 eV) the photoconductivity step, observed at about 9.2 eV. The figure implies that the step is nearly as steep in the liquid as in the two solid samples drawn for comparison. At somewhat higher photon energies (≈ 9.5 eV in the solid and ≈ 9.4 eV in the liquid) a dip is seen in the curve, while at higher energies no further structure could be ascertained. Comparing various liquid samples, both the position and the depth of the dip is well reproducible. In solid samples the depth of the dip varies from sample to sample, though its position does not change. A systematic investigation of this point has not been made, but, in general, samples observed at higher temperatures have more pronounced dips. It seems that this is connected with the better quality of the high-temperature crystals.

Electron energies characteristic to the photoconductivity excitation spectra along with related quantities obtained from the reflection spectrum appear in Table I. The close relationship between the exciton-series limit and the onset of photoconduction is obvious. Moreover, it is seen that the dip in the excitation spectrum is related to the $E_1[\Gamma(\frac{1}{2})]$ exciton. The implications of Table I for the correct value of the energy gap $E_G[\Gamma(\frac{3}{2})]$ will be discussed now.

In principle the exciton-series limit $E_\infty[\Gamma(\frac{3}{2})]$ should be equal to the energy gap E_G. The photoconductivity threshold E_{pc} is somewhat less reliable, since photoconductivity may start at photon energies sufficient to create high-order ($n \geq 3$) Wannier excitons and these may dissociate thermally or on surfaces. Thus, according to Table I, $E_G[\Gamma(\frac{3}{2})] = 9.278 \pm 0.005$ eV for solid xenon at 130 °K, and the difference of 0.013 eV between this value and E_{pc} is attributed to photoconductivity due to high-order excitons.

The above considerations bear significance for the determination of the band gap of the liquid. In the solid, $E_\infty[\Gamma(\frac{3}{2})]$ is calculated from the observed values of $E_2[\Gamma(\frac{3}{2})]$ and $E_3[\Gamma(\frac{3}{2})]$. The value of the observed $E_1[\Gamma(\frac{3}{2})]$ is not used and it does not fit the Wannier formula $E_n = E_\infty - G/n^2$, $n = 1, 2, \ldots,$ since central cell corrections[18, 19] have to be applied. However, in the liquid only $E_1[\Gamma(\frac{3}{2})]$ and $E_2[\Gamma(\frac{3}{2})]$ are observed and thus $E_\infty[\Gamma(\frac{3}{2})]$ had to be calculated from these peaks. Since the central cell corrections for the liquid have not been calculated, the values $E_\infty[\Gamma(\frac{3}{2})]$ of Table I cannot be confidently put equal to $E_G[\Gamma(\frac{3}{2})]$. On the other hand, an independent determination of $E_G[\Gamma(\frac{3}{2})]$ can be made using the value $E_{pc} = 9.202$ eV and adding to it 0.013 eV, i.e., the difference $E_G[\Gamma(\frac{3}{2})] - E_{pc}$ in the solid; this yields $E_G[\Gamma(\frac{3}{2})] = 9.225$ eV for liquid xenon. On the basis of all the above evidence, we shall take $E_G[\Gamma(\frac{3}{2})] = 9.22 \pm 0.01$ eV.

It should be emphasized that this result definitely differs from those by Robert and Wilson[17] $\{E_G[\Gamma(\frac{3}{2})] = 8.9 \text{ eV}\}$. The graphs by these authors are based

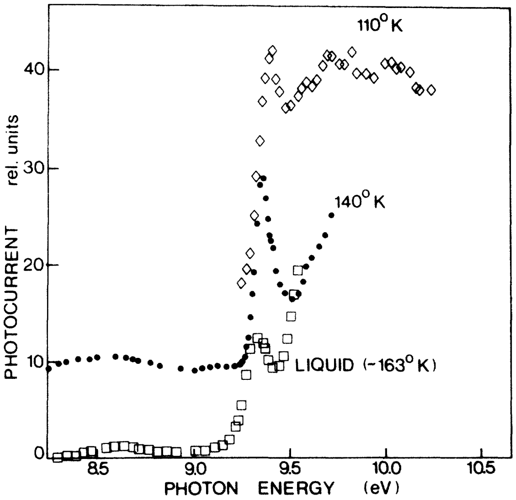

FIG. 1. Photocurrent, normalized to equal numbers of incident photons, as a function of photon energy. For clarity, the plots are staggered vertically. The 110 and 140 °K plots refer to the solid. The data of the lower two plots were obtained with a krypton-filled Tanaka lamp, those of the uppermost one with an argon-filled lamp.

on a set of measurements taken at a small set of wavelengths. The measurements were plagued by impurities in the liquid and probably also by photoemission from various parts of the sample cell. On the other hand, there is a satisfactory correlation between the present results and those obtained by Spear and Le Comber.[20]

IV. DISCUSSION

A. Photoconduction versus excitonic transitions

It was shown above that there is a very good agreement between the optically determined band gap and that determined from the onset of photoconductivity. Accordingly, the photoconduction at this step and beyond it can be attributed to transitions from the uppermost valence band to the conduction band ($\Gamma_8^- \rightarrow \Gamma_6^+$ in the solid, corresponding to the $5s^2 5p^6\,{}^1S_0 \rightarrow 5s^2 5p^5 6s^1\,{}^3P_1$ atomic transition). The dip of the photoconductivity versus photon-energy curve (at 9.5 eV in the solid and at 9.45 eV in the liquid) is very close to the $n=1$ exciton peak belonging to transitions from the deeper spin-orbit split valence band to the conduction band. The obvious explanation of this fact is the assumption that the absorption coefficient increases considerably when the photon energy suffices to create the exciton in question $\{$denoted as $n=1\ [\Gamma(\frac{1}{2})]\}$, and thus less photons per second are available for the creation of conduction band electrons. When considering the kinetics of the processes, it should be noted that $n=1\ [\Gamma(\frac{1}{2})]$ excitons may decompose thus creating conduction electrons. It follows from these considerations that absorption due to band-to-band ($\Gamma_8^- \rightarrow \Gamma_6^+$) transitions is about equal to or somewhat weaker than that attributable to the creation of this exciton. This conclusion is in full accord with the well-known fact that no optical absorption edge is observed in the rare-gas solids, because of the strong absorption ($\alpha \approx 10^6$ cm^{-1}) due to the excitonic transitions.

B. Forbidden band, exciton rydberg, and effective mass in liquid and solid xenon

It was shown[13] that the temperature dependence of the exciton peak positions in solid xenon can be attributed to the concurrent change in density. Moreover, exciton peak positions in the liquid were found to fit extrapolated portions of the linear plots representing the density dependence of the exciton peak positions of the solid. These results have suggested that the exciton peak positions are primarily determined by the (average) distance between nearest neighbor atoms. On the basis of the present results it is possible to test whether the same statement is true about the parameters used for the description of the exciton position in the one-electron effective-mass model, namely, the band gap E_G, the exciton rydberg G, and the reduced effective exciton mass m^*_{exc}. The results are as follows: Extrapolation of the straight lines E_G versus the density of the solid to the density of the liquid yields 9.24 eV, while the energy gap in the liquid is 9.22 eV. The extrapolation of the exciton rydberg G to the density of the liquid is 1.21 eV, compared with the actual value of 1.084 eV. Regarding m^*_{exc}, the extrapolated value in terms of free-electron mass is 0.31, while the experimental value is 0.27. [The comparisons were made on the basis of Marcoux's measurements[21, 22] of the low-frequency dielectric constant in liquid and solid Xe and the Clausius-Mosotti relationship for the density dependence of ϵ. An alternative procedure would be to use the temperature-dependent results on ϵ of the solid by Smith and Sinnock[23] and use Marcoux's ϵ for the liquid. Such a procedure yields an even larger discrepancy

TABLE I. Exciton series limit $E_\infty[\Gamma(\frac{3}{2})]$, photon energy at the onset of photoconduction E_{pc}, the position $E_1[\Gamma(\frac{1}{2})]$ of the $n=1$ peak of the $\Gamma(\frac{1}{2})$ series and the position E_D of the photocurrent dip in solid and liquid xenon, all in electron volts.

	$E_\infty[\Gamma(\frac{3}{2})]$	E_{pc}	$E_1[\Gamma(\frac{1}{2})]$	E_D
Solid Xe, ≈130 °K	9.278 ± 0.005 [a]	9.265 ± 0.005 [b]	9.462 ± 0.005 [a]	9.50 ± 0.01 [c]
Liquid Xe, ≈163 °K	9.22 ± 0.02 [d] 9.23 ± 0.02 [f]	9.202 ± 0.005 [e]	9.37 ± 0.02 [a]	9.45 ± 0.01 [c]

[a] From the data of Ref. 13.

[b] Average on seven samples, present work.

[c] Present work.

[d] Calculated from $E_2[\Gamma(\frac{3}{2})]$ and $E_1[\Gamma(\frac{3}{2})]$ (Ref. 13), without central cell correction.

[e] Average on six samples, present work.

[f] Calculated from $E_2[\Gamma(\frac{3}{2})]$ and $E_1[\Gamma(\frac{3}{2})]$ (Ref. 13), using the same central cell correction for $E_1[\Gamma(\frac{3}{2})]$ as in the solid ($\Delta E_1 = -0.036$ eV).

(by 15%) between the extrapolated and the actual values of m^*_{exc} for the liquid.] Thus there is a small, but clear discrepancy in the case of E_G and discrepancies by more than 10% for G and m^*_{exc}. A consistent uniform theoretical description of the Wannier excitons in the liquid as well as in the solid, not based on the one-electron, effective-mass model, would be useful for the explanation of these facts.

C. Transport parameters

Using values of parameters measured by other authors in combination with the above results a set of further parameters was determined. The measured values[1] of the electron mobility μ_e and the effective mass m^* determined in this work yield the momentum relaxation time τ_p,

$$\tau_p = \mu_e m^*/e\,. \tag{1}$$

For the calculations, we assumed an infinite hole mass and thus the exciton reduced effective mass, determined from the above optical and photoconductivity measurements, could be equated with the electron effective mass. The mean free path L_p determining the momentum transfer rate was obtained as follows:

$$L_p = (kT/m^*)^{1/2}\tau_p\,. \tag{2}$$

In order to find the scattering length a in the framework of effective range theory the scattering cross section σ of an atom was approximated by

$$\sigma = 4\pi a^2 S(0)\,, \tag{3}$$

$S(0)$ being the structure factor: this, in turn, was determined by means of the Ornstein-Zernike formula[24]

$$S(0) = kT/\beta\Omega_0\,, \tag{4}$$

β being the bulk modulus and Ω_0 the atomic volume. Using $L_p = \Omega_0/\sigma$ one obtains

$$a = [(1/L_p)\beta\Omega_0^2/4\pi kT]^{1/2}\,. \tag{5}$$

This formula may serve for the determination of the absolute value of a; finally the deformation potential $E_{1\text{CB}}$ is given by[24]

$$E_{1\text{CB}} = ah^2/2\pi\Omega_0 m^*\,. \tag{6}$$

Values of E_G, G, m^*, E, μ, τ_p, L_p, a, and $E_{1\text{CB}}$ for both the liquid and the 161 °K solid are compiled in Table II. It is seen that the mean free path and the relaxation time in the solid are about twice as large as in the liquid. The values of a are very near to each other in both cases, the same being true for $E_{1\text{CB}}$.

For a systematic discussion of Table II, an electron-transport theory in the liquid, dealing in full with the effective mass, would be needed. For example, there does not seem to be any simple explanation for the fact that m^* in the liquid is smaller than that in the solid by more than 10%. The concept of effective mass has not been incorporated in the advanced transport theories, applicable to liquid rare gases, as put forward by Lekner,[27] Cohen and Lekner[28] and by Springett, Jortner and Cohen.[29] Because of this, Table II contains data (E_G, G, m^*, L, and τ) calculated from one-electron, effective mass models of the Wannier exciton and of the electronic mobility, as well as data (on a and $E_{1\text{CB}}$) calculated on the basis of the effective range scattering theory which was originally formulated for gases and thus did not incorporate the effective-mass concept.[30]

An estimate for the upper bond of the systematic error introduced by this procedure can be made by changing m^* to m_e, the free electron mass, in the formulas for a and $E_{1\text{CB}}$. Such a substitution decreases the value of $|a|$ to 3×10^{-9} cm and $|E_{1\text{CB}}|$ to 0.2 eV in the liquid, with similar changes in the solid. Thus, neglecting the difference between the effective mass and the free electron mass is not justified.

The value of $|a|$ obtained in liquid and solid xenon ($|a| \simeq a_0$, a_0 being the Bohr radius) differs considerably from that obtained for the gas, namely $a = -6.5a_0$.[30] The present results do not yield the sign of the scattering length. For liquid Ar, Lekner[27] took into account local fields caused by

TABLE II. Comparison of transport parameters in solid and liquid xenon. Values of other data used in the calculations are also quoted.

	Solid T = 161.2 °K	Liquid T = 163 °K	Unit
E_G	9.272	9.22	eV
G	1.063	1.084	eV
ϵ_∞	2.00 [a]	1.85 [b]	...
m^*	0.31 [c]	0.27	electron mass
μ	4.5×10^3 [d]	2.2×10^3 [e]	$\text{cm}^2\,\text{V}^{-1}\,\text{sec}^{-1}$
τ_p	8.0×10^{-13}	3.4×10^{-13}	sec
L	7.1×10^{-6}	3.3×10^{-6}	cm
β	1.36×10^{10} [f]	0.58×10^{10} [g]	dyn/cm^2
$\lvert a\rvert$	3.8×10^{-9}	4.2×10^{-9}	cm
$\lvert E_{1\text{CB}}\rvert$	0.93	1.01	eV

[a] Reference 22.

[b] Reference 21.

[c] This value is smaller by about 10% than that of Ref. 13, since $\epsilon = n_D^2$ was assumed in Ref. 13, n_D being the refractive index for sodium light.

[d] Reference 1, at 157 °K.

[e] Reference 1.

[f] Reference 25.

[g] Reference 26.

induced dipoles and found that a should be $+1.44a_0$ instead of $-1.5a_0$ in the gas. Moreover, the Ramsauer minimum, well known and prominent in the gas, disappears in the liquid according to Lekner's calculation because of correlation between the scattering centers. It would be rather interesting to work through a similar calculation for liquid and solid xenon as well, since, on the basis of the present data, direct comparison between measured and calculated scattering lengths would be possible. The theory would also reveal whether the Ramsauer minimum does exist in liquid xenon.

For the deformation potentials E_{1CB} the only comparison that can be made is with that of Druger,[31] based on the analysis of the mobility. According to his estimate, $E_{1CB} = 1.4$ eV. In view of the widely different nature of the estimates and approximations involved, the agreement is satisfactory.

V. CONCLUSIONS

The combination of results from photoconductivity excitation spectra and mobility and isothermal compressibility data yields a series of transport-parameter data for both solid and liquid xenon. It is apparent from the data that liquid xenon is a normal photoconductor with no indications of electron localization. The results point to a considerable decrease of the absolute value of the scattering length in the condensed phases when compared with that of the gas. Application of Lekner's theory to the condensed xenon phases would both serve as a further test for the theory, as well as resolve the question of whether or not there is a Ramsauer minimum in these systems. A study of zero-field mobilities in a wide range of temperature and pressure, as performed for liquid argon,[32] would yield a fuller understanding of electron transport in liquid xenon as well.

---

[*] Work sponsored in part by the Central Research Fund of the Hebrew University.

[1] L. S. Miller, S. Howe, and W. E. Spear, Phys. Rev. 166, 871 (1968).

[2] B. Raz and J. Jortner, Chem. Phys. Lett. 4, 511 (1970).

[3] B. Raz and J. Jortner, Proc. R. Soc. Lond. A 317, 113 (1970).

[4] A. Gedanken, Z. Karsch, B. Raz, and J. Jortner, Chem. Phys. Lett. 20, 163 (1973).

[5] G. Baldini, Phys. Rev. 137, A508 (1965).

[6] A. Gedanken, B. Raz, and J. Jortner, J. Chem. Phys. 58, 1178 (1973).

[7] D. Beaglehole, Phys. Rev. Lett. 15, 551 (1965).

[8] U. Asaf and I. T. Steinberger, Phys. Lett. A 34, 204 (1971).

[9] G. Baldini, Phys. Rev. 128, 1562 (1962).

[10] I. T. Steinberger, C. Atluri, and O. Schnepp, J. Chem. Phys. 52, 2723 (1970).

[11] R. Haensel, G. Keitel, E. E. Koch, M. Skibowski, and P. Schreiber, Opt. Commun. 2, 59 (1970).

[12] J. Jortner, N. R. Kestner, S. A. Rice, and M. H. Cohen, J. Chem. Phys. 43, 2614 (1965).

[13] I. T. Steinberger and U. Asaf, Phys. Rev. B 8, 914 (1973).

[14] R. Haensel, G. Keitel, E. E. Koch, M. Skibowski, and P. Schreiber, Phys. Rev. Lett. 23, 1160 (1969).

[15] R. Haensel, G. Keitel, E. E. Koch, N. Kosuch, and M. Skibowski, Phys. Rev. Lett. 25, 1281 (1970).

[16] U. Asaf and I. T. Steinberger, Phys. Lett. A 41, 19 (1972).

[17] I. Roberts and E. G. Wilson, J. Phys. C 6, 2169 (1973).

[18] J. Hermanson and J. C. Phillips, Phys. Rev. 150, 652 (1967).

[19] J. Hermanson, Phys. Rev. 150, 660 (1967).

[20] W. E. Spear and P. G. Le Comber (private communication).

[21] J. Marcoux, Can. J. Phys. 48, 244 (1970).

[22] J. Marcoux, Can. J. Phys. 48, 1947 (1970).

[23] A. C. Sinnock and B. L. Smith, Phys. Lett. A 28, 22 (1968).

[24] N. F. Mott and E. A. Davis, *Electronic Processes in Noncrystalline Materials* (Clarendon, Oxford, 1971), Chap. 3.

[25] G. L. Pollack, Rev. Mod. Phys. 36, 748 (1964).

[26] Yu. P. Blagoi and V. A. Sorokin, Russ. J. Phys. Chem. 44, 1563 (1970).

[27] J. Lekner, Phys. Rev. 158, 130 (1967).

[28] M. H. Cohen and J. Lekner, Phys. Rev. 158, 305 (1967).

[29] B. E. Springett, J. Jortner, and M. H. Cohen, J. Chem. Phys. 48, 2720 (1968).

[30] T. O'Malley, Phys. Rev. 130, 1020 (1963).

[31] S. D. Druger, J. Chem. Phys. 54, 2339 (1971).

[32] J. A. Jahnke, L. Meyer, and S. A. Rice, Phys. Rev. A 3, 734 (1971).